

Tau polarizations in the three-body slepton decays with stau as the next lightest supersymmetric particle

Chih-Lung Chou* and Chung-Hsien Chou†

Institute of Physics, Academia Sinica, Nankang, Taipei, Taiwan 11529

(Received 19 March 2001; published 5 September 2001)

In the gauge-mediated supersymmetry breaking models with a scalar tau as the next-to-lightest supersymmetric particle, a scalar lepton may decay dominantly into its superpartner, the tau lepton, and the lightest scalar tau particle through $\tilde{l} \rightarrow l \tau^\pm \tilde{\tau}_1^\mp$. We give detailed formulas for the three-body decay amplitudes and the polarization asymmetry of the outgoing tau lepton. We find that the tau polarizations are sensitive to the model parameters such as the stau mixing angle, the neutralino to slepton mass ratio, and the neutralino mixing effect.

DOI: 10.1103/PhysRevD.64.075008

PACS number(s): 14.80.Ly, 12.60.Jv, 14.65.Ha

I. INTRODUCTION

Supersymmetry provides a natural solution to the hierarchy problem that associates with weak scale physics and Planck scale physics [1]. If nature is supersymmetric, it must spontaneously break supersymmetry and transmit the message to low-energy effective models. Two approaches are widely considered to satisfy the message transmitting strategy. One is the gravity mediation approach which has the supersymmetry breaking scale \sqrt{F} about order 10^{11} GeV [2,3]. The gravitino mass is typically much larger than those of gauginos and sfermions under this framework. Because of the largeness of \sqrt{F} , the gravitino interaction is also too weak to play important roles in collider phenomenology. Another approach uses gauge interactions to mediate the supersymmetry breaking effect [4,5]. In the gauge-mediated supersymmetry breaking (GMSB) scenarios, the supersymmetry breaking scale \sqrt{F} is sufficiently small so that the gravitino \tilde{G} is always the lightest supersymmetric particle (LSP) with mass

$$m_{\tilde{G}} = \frac{F}{\sqrt{3}M_{Pl}} = 2.37 \times 10^{-4} \times \left(\sqrt{\frac{F}{1 \text{ TeV}}} \right)^2 \text{ eV}, \quad (1)$$

where M_{Pl} denotes the reduced Planck scale $\sim 2.4 \times 10^{18}$ GeV. Since the soft masses of other superparticles are associated with the weak scale in the GMSB models, within a typical range of \sqrt{F} , the gravitino is far lighter than other superparticles and becomes the LSP.

It is well known that different scenarios for the next-to-lightest supersymmetric particle (NLSP) in the GMSB models could be crucial in discovering supersymmetry signals in colliders and may lead to different phenomenologies. In the neutralino NLSP scenarios, the lightest neutralino \tilde{N}_1 decays into a photon and a gravitino which carries missing energy and escapes the detectors [6]. If the supersymmetric (SUSY) breaking scale \sqrt{F} is less than a few thousand TeV, the neutralino decay $\tilde{N}_1 \rightarrow \gamma \tilde{G}$ would be prompt enough to occur within the detector. One can therefore use inclusive $\gamma\gamma + \cancel{E}_T + X$ signals in detecting supersymmetry. In the slepton

NLSP scenarios, the lightest slepton can promptly decay into its partner and a gravitino with a sufficiently small scale \sqrt{F} [7]. Depending on the scale \sqrt{F} , the slepton NLSP may live long enough to leave tracks and kinks in detectors. In general, other NLSP scenarios are also plausible depending upon the various constructions of supersymmetry breaking models.

Scalar leptons can be easily found at future linear e^+e^- colliders if it is kinematically allowed [8]. By measuring their masses and decay distributions one could determine some of the minimal supersymmetric standard model (MSSM) parameters. The phenomenology of sleptons in future linear colliders then deserves detailed study.

In this paper we concentrate on the GMSB scenarios in which the lighter scalar tau lepton (stau) $\tilde{\tau}_1$ is the NLSP. In general, we can write down the stau mass eigenstates $\tilde{\tau}_1$ and $\tilde{\tau}_2$ in terms of the stau mixing angle $\theta_{\tilde{\tau}}$:

$$\tilde{\tau}_1 = \cos \theta_{\tilde{\tau}} \tilde{\tau}_L + \sin \theta_{\tilde{\tau}} \tilde{\tau}_R, \quad (2)$$

$$\tilde{\tau}_2 = -\sin \theta_{\tilde{\tau}} \tilde{\tau}_L + \cos \theta_{\tilde{\tau}} \tilde{\tau}_R, \quad (3)$$

where $\theta_{\tilde{\tau}}$ ranges from $0 \leq \theta_{\tilde{\tau}} < \pi$. Since the mixing is proportional to fermion Yukawa coupling, due to the small mixing effects for scalar electrons (selectrons) and for scalar muons (smuons), the lightest selectron \tilde{e}_1 and the lightest smuon $\tilde{\mu}_1$ are nearly right-handed sleptons with almost equal masses. We will use \tilde{e}_R and $\tilde{\mu}_R$ to represent the lighter selectron and smuon, respectively, in this paper.

$\tilde{\tau}_1$ can decay into a tau lepton and a gravitino \tilde{G} in the detectors if the SUSY scale \sqrt{F} is not too large. If the scale \sqrt{F} is sufficiently large, the stau NLSPs may live long enough to leave tracks or kinks in the collider detectors. In many of the GMSB models, the lighter selectron and the lighter smuon are merely right-handed sleptons with nearly degenerate masses. Unlike $\tilde{\tau}_1$, they can decay not only through the two-body processes $\tilde{e}_R \rightarrow e \tilde{G}$ and $\tilde{\mu}_R \rightarrow \mu \tilde{G}$, but also through the processes such as $\tilde{l}_R \rightarrow l \tilde{N}_1$, $\tilde{l}_R \rightarrow \nu_l \tilde{\nu}_\tau \tilde{\tau}_1$, and $\tilde{l}_R \rightarrow l \tau \tilde{\tau}_1$ depending upon the model parameters. For instance, $\tilde{l}_R \rightarrow l \tau \tilde{\tau}_1$ will be kinematically forbidden if the

*Email address: choucl@phys.sinica.edu.tw

†Email address: chouch@phys.sinica.edu.tw

mass difference ($m_{\tilde{\tau}_R} - m_{\tilde{\tau}_1}$) is smaller than the tau mass m_τ . This could happen in the so-called slepton co-NLSP scenarios [9].

However, in the stau NLSP scenarios, there exists some parameter space where the three-body processes $\tilde{\tau}_R \rightarrow l\tau\tilde{\tau}_1$ could dominate over the two-body processes $\tilde{\tau}_R \rightarrow l\tilde{G}$ and lead to different signatures in colliders [10].

If the decay $\tilde{\tau}_1 \rightarrow \tau\tilde{G}$ takes place outside the detector, then one can directly identify the stau tracks or decay kinks. Thus in the e^+e^- colliders, the pair-produced sleptons may decay in collider detectors through $e^+e^- \rightarrow \tilde{\tau}_R^+ \tilde{\tau}_R^- \rightarrow l^+ l^- \tau\tau\tilde{\tau}_1\tilde{\tau}_1$. In the e^-e^- colliders, right-handed sleptons are produced through the t -channel processes and then decay as $e^-e^- \rightarrow \tilde{\tau}_R^- \tilde{\tau}_R^- \rightarrow l^- l^- \tau\tau\tilde{\tau}_1\tilde{\tau}_1$. It is also found that \tilde{e}_R and $\tilde{\mu}_R$ could have macroscopic decay lengths that are smaller than the dimensions of typical detectors if the mass difference $|m_{\tilde{\tau}_R} - m_\tau - m_{\tilde{\tau}_1}|$ is suitably small. If this is the case, the secondary vertices of the three-body processes could be resolved and each $\tilde{\tau}_1$ particle can be identified as coming from one of the pair-produced selectrons or smuons. In this case one could measure the polarizations of the τ leptons. The τ polarization provides another observable that could help to pin down the stau mixing angle and/or the ratio of the neutralino and the slepton masses.

However, there might be the possibility that the two-body and three-body decay modes are of comparable amplitudes and can therefore decay in the detector. In this case we might have the decay process $e^-e^+ \rightarrow \tilde{\tau}_R^- \tilde{\tau}_R^+ \rightarrow l^- l^+ \tau^\pm \tilde{\tau}_1^\mp \tilde{E} \rightarrow l^- l^+ \tau^\pm \tau^\mp \tilde{E}\tilde{E}$, i.e., two tau leptons with opposite charges in the final state. One of the tau leptons is coming from the three-body decay of the slepton, therefore its kinetic energy is less than $|m_{\tilde{\tau}_R} - m_\tau - m_{\tilde{\tau}_1}|$. The other tau lepton is from the two-body decay of the scalar tau and hence carries larger momentum and is much harder than the tau lepton originated from the three-body decay. In this interesting case we can easily identify the softer tau lepton from the three-body decay from $\tilde{\tau}_R$.

Motivated by the above observation, we calculate the polarizations for the tau leptons in the three-body decays $\tilde{\tau}_R \rightarrow l\tau^\pm \tilde{\tau}_1^\pm$ in the paper. It is expected that the tau polarizations should depend on the stau mixing angle and the mass

ratio $m_{\tilde{N}_1}/m_{\tilde{e}_R}$. In Sec. II of this paper we set the notations and give formulas for the polarizations of the tau leptons in the three-body slepton decays. Numerical results are presented and discussed in Sec. III. In Sec. IV we make our conclusion.

II. THREE-BODY SLEPTON DECAYS

As mentioned in the preceding section, the three-body decays $\tilde{\tau}_R \rightarrow l\tau\tilde{\tau}_1$ could dominate over the two-body decays $\tilde{\tau}_R \rightarrow l\tilde{G}$ in some parameter space if the SUSY breaking scale \sqrt{F} is sufficiently large. We restrict the scenario where the two-body processes $\tilde{e}_R \rightarrow e + \tilde{N}_i$ are forbidden, i.e., we assume the following mass relation:

$$m_e + m_{\tilde{N}_i} > m_{\tilde{e}_R} > m_e + m_\tau + m_{\tilde{\tau}_1}. \quad (4)$$

Therefore the only competing decay processes for \tilde{e}_R and $\tilde{\mu}_R$ are $\tilde{\tau}_R \rightarrow l\tau^\pm \tilde{\tau}_1^\pm$.

Because of the invariance of charge conjugation and parity transformation, we can write down the following identities for the selectron decays:

$$\Gamma(\tilde{e}_R^+ \rightarrow e^+ \tau_R^\pm \tilde{\tau}_1^\mp) = \Gamma(\tilde{e}_R^- \rightarrow e^- \tau_L^\mp \tilde{\tau}_1^\pm), \quad (5)$$

$$\Gamma(\tilde{e}_R^+ \rightarrow e^+ \tau_L^\pm \tilde{\tau}_1^\mp) = \Gamma(\tilde{e}_R^- \rightarrow e^- \tau_R^\mp \tilde{\tau}_1^\pm), \quad (6)$$

where L (R) denotes the left (right) helicity for the tau leptons in the decay processes. Therefore we will only discuss the decays of \tilde{e}_R^+ .

At tree level, the selectron \tilde{e}_R decays through the propagation of B -ino \tilde{B} and W -ino \tilde{W}^3 . Since B -ino \tilde{B} , W -ino \tilde{W}^3 , and the two neutral Higgsinos $\tilde{h}_1^0, \tilde{h}_2^0$ can mix and form the neutralino mass eigenstates \tilde{N}_i , it is appropriate to do the calculation in terms of the neutralino parameters. On the basis of $\psi_i = (\tilde{B}, \tilde{W}^3, i\tilde{h}_1^0, i\tilde{h}_2^0)$, the neutralino states and the associated diagonal mass matrix M_D are given by

$$\tilde{N}_i = (V^+)_{ij} \psi_j, \quad (7)$$

$$M_D = V^+ M V. \quad (8)$$

Here V denotes the transforming matrix which diagonalizes the neutralino mass matrix M :

$$M = \begin{pmatrix} m_1 & 0 & m_Z \sin \theta_W \cos \beta & -m_Z \sin \theta_W \sin \beta \\ 0 & m_2 & -m_Z \cos \theta_W \cos \beta & m_Z \cos \theta_W \sin \beta \\ m_Z \sin \theta_W \cos \beta & -m_Z \cos \theta_W \cos \beta & 0 & -\mu \\ -m_Z \sin \theta_W \sin \beta & m_Z \cos \theta_W \sin \beta & -\mu & 0 \end{pmatrix}, \quad (9)$$

where m_Z is the mass of the Z boson, m_1 denotes the soft breaking mass of B -ino \tilde{B} , m_2 is the soft breaking mass of W -ino \tilde{W}^3 , θ_W denotes the weak Weinberg angle, $\tan \beta$ is the ratio between the vacuum expectation values of the two

Higgs doublets in the model, and μ is the supersymmetric Higgs mass parameter.

In our study the tau polarizations are measured in the laboratory frame. When the collider beam energy is threshold

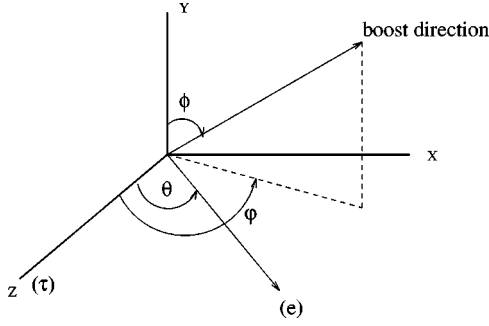


FIG. 1. The selectron boost direction (ϕ, φ) in the laboratory frame where the electron moving direction and the tau moving direction spans the XZ plane. Here θ denotes the angle between the outgoing electron and the outgoing tau lepton.

to produce the selectrons in pairs, the selectrons may travel with velocity v before decay and thus experience a boost which is characterized by the boost factor $\gamma = (v/c)/\sqrt{1-(v/c)^2}$. Figure 1 shows the selectron boost direction in the laboratory frame. The moving direction of the outgoing tau lepton is assigned the Z direction and the XZ plane is spanned by the outgoing electron and the tau lepton. By summing all tree-level contributions for the decay $\tilde{e}_R^+ \rightarrow e^+ \tau^- \tilde{\tau}_1^+$, the transition amplitudes $|im_{(L,R)}^-|^2$ for different helicities (L,R) of the tau final states are given by

$$|im_{(R)}^-|^2 = \left| \sum_{j=1}^4 \frac{2Q_e V_{Rj}^* \sqrt{E_e}}{(q^2 - m_{\tilde{N}_j}^2)} \left\{ (C_{1j} E_{\tilde{e}_R}^- \sqrt{E+K} - C_{2j}^* m_{\tilde{N}_j} \sqrt{E-K}) \cos \frac{\theta}{2} + C_{1j} P_{\tilde{e}_R}^- \sqrt{E+K} \left(\sin \phi \sin \varphi \sin \frac{\theta}{2} + \sin \phi \cos \varphi \cos \frac{\theta}{2} - i \cos \phi \sin \frac{\theta}{2} \right) \right\} \right|^2, \quad (10)$$

$$|im_{(L)}^-|^2 = \left| \sum_{j=1}^4 \frac{2Q_e V_{Rj}^* \sqrt{E_e}}{(q^2 - m_{\tilde{N}_j}^2)} \left\{ (C_{1j} E_{\tilde{e}_R}^- \sqrt{E-K} - C_{2j}^* m_{\tilde{N}_j} \sqrt{E+K}) \sin \frac{\theta}{2} + C_{1j} P_{\tilde{e}_R}^- \sqrt{E-K} \left(\sin \phi \sin \varphi \cos \frac{\theta}{2} - \sin \phi \cos \varphi \sin \frac{\theta}{2} + i \cos \phi \cos \frac{\theta}{2} \right) \right\} \right|^2, \quad (11)$$

where

$$q^2 \equiv m_{\tilde{e}_R}^2 - 2PE_{\tilde{e}_R}^- - 2PP_{\tilde{e}_R}^- \sin \phi \cos(\theta - \varphi), \quad (12)$$

$(E_{\tilde{e}_R}^-, P_{\tilde{e}_R}^-)$ and (E, K) denote the (energy, momentum) pairs of the right-handed selectron and the outgoing tau lepton in the laboratory frame, respectively, P is the outgoing electron energy, $m_{\tilde{e}_R}^-$ and $m_{\tilde{N}_j}$ denote the masses of the right-handed selectron and the j th neutralino respectively, Q_e represents the electric coupling of electron, and the coefficients C_{1j}, C_{2j} , and V_{Rj} are given by [11]

$$V_{Lj} = \frac{1}{2 \sin \theta_W} V_{2j} + \frac{1}{2 \cos \theta_W} V_{1j}, \quad (13)$$

$$V_{Rj} = \frac{1}{\cos \theta_W} V_{1j}, \quad (14)$$

$$C_{1j} = \lambda_\tau V_{3j} \cos \theta_{\tilde{\tau}} - \sqrt{2} Q_e V_{Rj} \sin \theta_{\tilde{\tau}}, \quad (15)$$

$$C_{2j} = \lambda_\tau V_{3j} \sin \theta_{\tilde{\tau}} + \sqrt{2} Q_e V_{Lj} \cos \theta_{\tilde{\tau}}. \quad (16)$$

Here λ_τ is the coupling strength for the tau Yukawa coupling term $\lambda_\tau H_1 L_\tau R_\tau$. Similarly, the decay process $\tilde{e}_R^+ \rightarrow e^+ \tau^+ \tilde{\tau}_1^-$ has the transition amplitudes

$$|im_{(R)}^+|^2 = \left| \sum_{j=1}^4 \frac{2Q_e V_{Rj}^* \sqrt{E_e}}{(q^2 - m_{\tilde{N}_j}^2)} \left\{ (-C_{1j}^* m_{\tilde{N}_j} \sqrt{E-K} + C_{2j} E_{\tilde{e}_R}^- \sqrt{E+K}) \cos \frac{\theta}{2} + C_{2j} P_{\tilde{e}_R}^- \sqrt{E+K} \left(\sin \phi \sin \varphi \sin \frac{\theta}{2} + \sin \phi \cos \varphi \cos \frac{\theta}{2} - i \cos \phi \sin \frac{\theta}{2} \right) \right\} \right|^2, \quad (17)$$

$$|im_{(L)}^+|^2 = \left| \sum_{j=1}^4 \frac{2Q_e V_{Rj}^* \sqrt{E_e}}{(q^2 - m_{\tilde{N}_j}^2)} \left\{ (-C_{1j}^* m_{\tilde{N}_j} \sqrt{E+K} + C_{2j} E_{\tilde{e}_R}^- \sqrt{E-K}) \sin \frac{\theta}{2} + C_{2j} P_{\tilde{e}_R}^- \sqrt{E-K} \left(\sin \phi \sin \varphi \cos \frac{\theta}{2} - \sin \phi \cos \varphi \sin \frac{\theta}{2} + i \cos \phi \cos \frac{\theta}{2} \right) \right\} \right|^2. \quad (18)$$

As easily seen from Eqs. (10)–(18), the amplitudes do depend upon the selectron boost angles and the selectron momentum $P_{\tilde{e}_R}^-$.

Taking into account the selectron boost effect, the decay rate $\Gamma_{L,R}$ of different tau lepton helicities L or R for \tilde{e}_R is obtained as

$$\Gamma_{(L,R)} = \int d\phi d\varphi F(\phi, \varphi) \Gamma_{(L,R)}(\phi, \varphi), \quad (19)$$

with

$$\Gamma_{(L,R)}(\phi, \varphi) \equiv \int \frac{dE d[\cos \theta]}{64\pi^3 E_{e_R}^-} \frac{KP |im_{(L,R)}|^2}{E_{e_R}^- - E + K \cos \theta - P_{e_R}^- \sin \phi (\sin \varphi \sin \theta + \cos \varphi \cos \theta)}, \quad (20)$$

$$P \equiv \frac{m_{e_R}^2 + m_{\tau}^2 - m_{\tilde{\tau}_1}^2 - 2EE_{e_R}^- + 2P_{e_R}^- K \sin \phi \cos \varphi}{2[E_{e_R}^- - E + K \cos \theta - P_{e_R}^- \sin \phi (\sin \varphi \sin \theta + \cos \varphi \cos \theta)]}, \quad (21)$$

where $F(\phi, \varphi)$ is the probability density function for selectron boosting in the (ϕ, φ) direction, E is the energy for the outgoing tau lepton, $K = \sqrt{E^2 - m_{\tau}^2}$ denotes the momentum of the tau lepton, P is the energy of the outgoing electron, and θ is the angle between the tau and the electron.

Naively, the decay rates with selectron boost effects may differ to those without selectron boost effects to the order of $O(\gamma)$, i.e., $O(P_{e_R}^-/E_{e_R}^-)$. On the other hand, the spinless nature of selectrons leads to the following symmetry for $F(\phi, \varphi)$:

$$\begin{aligned} F(\phi, \pm \varphi) &= F(\phi, \pi \pm \varphi) = F(\pi - \phi, \pm \varphi) \\ &= F(\pi - \phi, \pi \pm \varphi). \end{aligned} \quad (22)$$

Thus all terms that are linear in $\cos \varphi$ or $\sin \varphi$ should be canceled after integrating out the φ dependence. Consequently, by observing that

$$\sqrt{E_{rest} \pm K_{rest}} = \sqrt{E \pm K} \left\{ 1 \mp \frac{1}{2} \gamma \cos \varphi \sin \phi + O(\gamma^2) \right\}, \quad (23)$$

where E_{rest} (K_{rest}) denotes the energy (momentum) of the outgoing tau lepton in the selectron rest frame, the decay rates in Eq. (19) are actually different than those without selectron boost effects to the order of $O(\gamma^2)$. Therefore, we simply do all the calculations in the selectron rest frame in the rest of the paper.

III. TAU LEPTON POLARIZATION

The tau lepton polarization asymmetry can be defined as

$$P_{\tau} \equiv \frac{\langle \Gamma_R \rangle - \langle \Gamma_L \rangle}{\langle \Gamma_R \rangle + \langle \Gamma_L \rangle}. \quad (24)$$

We can easily calculate the asymmetry by using the formulas presented in Sec. II. From Eqs. (5) and (6) the CP invariance leads to the following relations for the tau polarization:

$$\begin{aligned} P_{\tau}(\tilde{e}_R^+ \rightarrow e^+ \tau^+ \tilde{\tau}_1^-) &= -P_{\tau}(\tilde{e}_R^- \rightarrow e^- \tau^- \tilde{\tau}_1^+), \\ P_{\tau}(\tilde{e}_R^+ \rightarrow e^+ \tau^- \tilde{\tau}_1^+) &= -P_{\tau}(\tilde{e}_R^- \rightarrow e^- \tau^+ \tilde{\tau}_1^-). \end{aligned} \quad (25)$$

Therefore, we calculate only $P_{\tau}(\tilde{e}_R^+ \rightarrow e^+ \tau^+ \tilde{\tau}_1^-)$ and $P_{\tau}(\tilde{e}_R^+ \rightarrow e^+ \tau^- \tilde{\tau}_1^+)$ and give the numerical results in this section.

Generally, the transition amplitudes and the associated decay rates presented in the preceding section are sensitive to the neutralino masses and mixing effects. For instance, by assuming the dominance of \tilde{N}_1 propagating in the tree-level decay processes in the B -ino-like lightest neutralino scenario, the amplitude functions in the limit $\Delta \equiv (m_{e_R}^- - m_{\tilde{\tau}_1}^-) \ll m_{e_R}^-$ are obtained approximately as

$$\begin{aligned} |im_{(R)}^-|^2 &\propto \left\{ E_e \left| m_{e_R}^- \sqrt{E+K} \sin \theta_{\tilde{\tau}} \right. \right. \\ &\quad \left. \left. + \frac{m_{\tilde{B}}}{2} \sqrt{E-K} \cos \theta_{\tilde{\tau}} \right|^2 \cos^2 \frac{\theta}{2} \right\}, \end{aligned} \quad (26)$$

$$\begin{aligned} |im_{(R)}^+|^2 &\propto \left\{ E_e \left| m_{\tilde{B}} \sqrt{E-K} \sin \theta_{\tilde{\tau}} \right. \right. \\ &\quad \left. \left. + \frac{m_{e_R}^-}{2} \sqrt{E+K} \cos \theta_{\tilde{\tau}} \right|^2 \cos^2 \frac{\theta}{2} \right\}, \end{aligned} \quad (27)$$

$$\begin{aligned} |im_{(L)}^-|^2 &\propto \left\{ E_e \left| m_{e_R}^- \sqrt{E-K} \sin \theta_{\tilde{\tau}} \right. \right. \\ &\quad \left. \left. + \frac{m_{\tilde{B}}}{2} \sqrt{E+K} \cos \theta_{\tilde{\tau}} \right|^2 \sin^2 \frac{\theta}{2} \right\}, \end{aligned} \quad (28)$$

$$\begin{aligned} |im_{(L)}^+|^2 &\propto \left\{ E_e \left| m_{\tilde{B}} \sqrt{E+K} \sin \theta_{\tilde{\tau}} \right. \right. \\ &\quad \left. \left. + \frac{m_{e_R}^-}{2} \sqrt{E-K} \cos \theta_{\tilde{\tau}} \right|^2 \sin^2 \frac{\theta}{2} \right\}. \end{aligned} \quad (29)$$

From Eqs. (26)–(29), it is easily seen that the polarization ratio P_{τ} is determined by the mass ratio $m_{\tilde{B}}/m_{e_R}^-$. In the purely right-handed $\tilde{\tau}_1$ limit ($\sin \theta_{\tilde{\tau}} = 1$), P_{τ} becomes

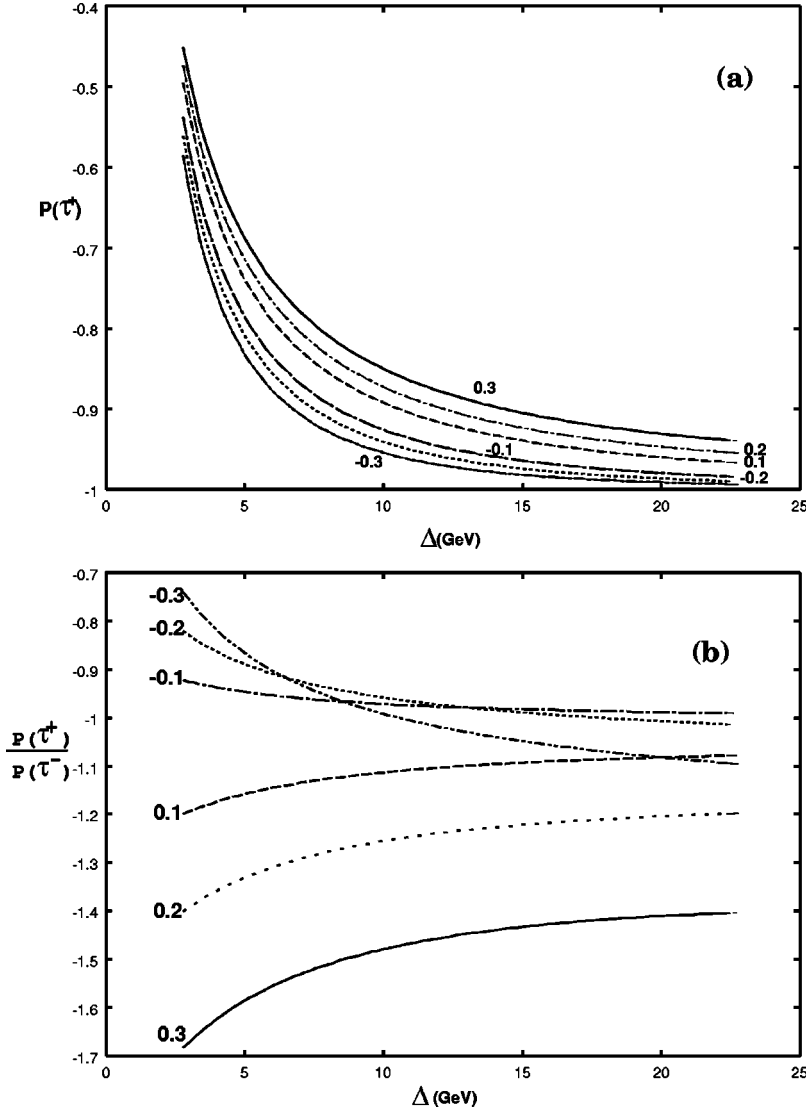


FIG. 2. Tau polarization as the function of Δ in the three-body decays of \tilde{e}_R with $r_{\tilde{B}}=2$ and $\cos \theta_{\tau^-} = -0.3, -0.2, -0.1, 0.1, 0.2, 0.3$. (a) $P_{\tau}(e_R^+ \rightarrow e^+ \tau^+ \tilde{\tau}_1^-)$ as a function of Δ . (b) The $P(\tau^+)/P(\tau^-)$ ratio as a function of Δ .

$$P_{\tau} \approx \pm \frac{\int_{m_{\tau}}^{\Delta} dE (E^2 - m_{\tau}^2) (\Delta - E)^2}{\int_{m_{\tau}}^{\Delta} dE E \sqrt{E^2 - m_{\tau}^2} (\Delta - E)^2} \quad (\pm) \text{ for } \tau^{\mp} \text{ final states.} \quad (30)$$

Equation (30) shows that the P_{τ} ratios always have opposite signs for τ^+ and τ^- production in the selectron decays, i.e., the $\tilde{e}_R^+ \rightarrow e^+ \tau^- \tilde{\tau}_1^+$ process tends to have right-handed tau leptons in the final states and the $\tilde{e}_R^+ \rightarrow e^+ \tau^+ \tilde{\tau}_1^-$ process tends to produce left-handed τ^+ 's in this limit.

The tau-lepton polarizations as the functions of the mass difference Δ with different $\cos \theta_{\tau^-}$ values are illustrated in Figs. 2(a) and 2(b) where the mass ratio $r_{\tilde{B}} \equiv m_{\tilde{B}}/m_{\tilde{e}_R} = 2$ is kept fixed. Although it was pointed out in [10] that when the mass differences between $\tilde{\tau}_1$ and \tilde{e}_R and $\tilde{\mu}_R$ are less than 10 GeV, the range of $\cos \theta_{\tau^-}$ will be within $0.1 \leq |\cos \theta_{\tau^-}| \leq 0.3$, we find that if we assume that $m_{\tilde{e}_R} \sim 200$ GeV the mass differences between $\tilde{\tau}_1$ and \tilde{e}_R and $\tilde{\mu}_R$ can be up to 20 GeV

while keeping $0.1 \leq |\cos \theta_{\tau^-}| \leq 0.3$. As shown in plot (a), $P(\tau^+) \equiv P_{\tau}(e_R^+ \rightarrow e^+ \tau^+ \tilde{\tau}_1^-)$ decreases as Δ increases. For a given Δ value, $P(\tau^+)$ always has larger values for larger $\cos \theta_{\tau^-}$ values. This could be explained by the fact that when $\cos \theta_{\tau^-}$ increases, the amplitude $|im_{(R)}^+|^2$ always increases faster than $|im_{(L)}^+|^2$ does when the mixing angle are within the range $0.1 \leq |\cos \theta_{\tau^-}| \leq 0.3$. Although not shown in the figure, from Eqs. (26) and (28) one can easily see that when Δ is kept fixed, a larger $\cos \theta_{\tau^-}$ will give smaller polarization $P(\tau^-) \equiv P_{\tau}(e_R^+ \rightarrow e^+ \tau^- \tilde{\tau}_1^+)$.

As shown in Fig. 2(b), the ratio between $P(\tau^+)$ and $P(\tau^-)$ is a slow varying function of Δ with fixed $r_{\tilde{B}}=2$ for most of the $\cos \theta_{\tau^-}$ range except for $\cos \theta_{\tau^-} = -0.3$. This is due to the complex interplay between the factors $\sqrt{E+K} \cos \theta_{\tau^-}$ and $\sqrt{E-K} \sin \theta_{\tau^-}$. When the mass difference Δ is small, $\sqrt{E+K}$ and $\sqrt{E-K}$ are comparable, and both $|im_{(R)}^+|^2$ and $|im_{(L)}^-|^2$ are getting smaller as $\cos \theta_{\tau^-}$ changing from -0.1 to -0.3 . On the other hand, when Δ goes larger, say $\Delta=20$ GeV, $\sqrt{E+K}$ is much larger than $\sqrt{E-K}$ and $|im_{(L)}^-|^2$ ($|im_{(R)}^+|^2$) is getting larger (smaller) as $\cos \theta_{\tau^-}$ changing from

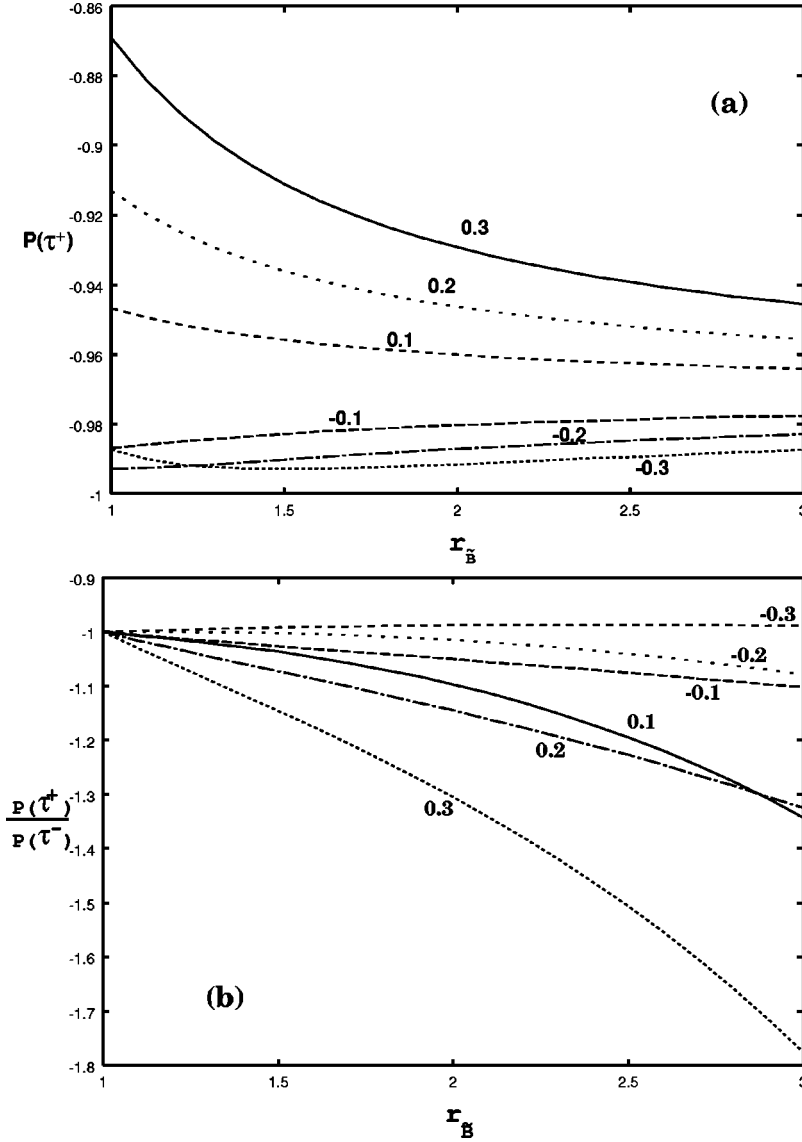


FIG. 3. Tau polarization as the function of the mass ratio $r_{\tilde{B}} \equiv m_{\tilde{B}}/m_{\tilde{e}_R}$ with seven choices $\cos \theta_{\tilde{\tau}} = -0.3, -0.2, -0.1, 0.1, 0.2, 0.3$, and $\Delta = 20$ GeV. (a) $P_{\tilde{\tau}}(e_R^+ \rightarrow e^+ \tau^+ \tilde{\tau}_1^-)$ as a function of $r_{\tilde{B}}$. (b) The $P(\tau^+)/P(\tau^-)$ ratio as a function of $r_{\tilde{B}}$.

-0.1 to -0.3. It thus leads to the intersections for those curves with negative $\cos \theta_{\tilde{\tau}}$ values.

Figures 3(a) and 3(b) show the mass ratio $r_{\tilde{B}}$ dependence of the tau polarizations. As shown in Fig. 3(a), $P(\tau^+)$ is a slow varying function of $r_{\tilde{B}}$ with fixed Δ value ($\Delta = 20$ GeV in the plot). However, the ratio $P(\tau^+)/P(\tau^-)$ varies significantly for $0.1 \leq \cos \theta_{\tilde{\tau}} \leq 0.3$ with a fixed Δ value as shown in Fig. 3(b). This plot may help in determining the model parameters such as $r_{\tilde{B}}$ and $\cos \theta_{\tilde{\tau}}$ in the B -ino-like lightest neutralino scenarios. For example, a ratio $P(\tau^+)/P(\tau^-) = -1.5$ will lead to $\cos \theta_{\tilde{\tau}} \approx 0.3$ and $r_{\tilde{B}} \geq 2.5$ in the model with $\Delta = 20$ GeV.

In Figs. 4(a)–4(c) we plot the tau polarization functions and their ratio as functions of $\cos \theta_{\tilde{\tau}}$ for $r_{\tilde{B}} = 2$ and five choices $\Delta = 4, 8, 12, 16, 20$ GeV. Figure 4(a) shows that the polarization $P(\tau^+)$ increases as $\cos \theta_{\tilde{\tau}}$ increases for the $\cos \theta_{\tilde{\tau}}$ range under consideration. Similar behaviors occur when varying the Δ value in the model. Usually a larger Δ value will imply a lower tau polarization for ($\tilde{e}_R^+ \rightarrow e^+ \tau^+ \tilde{\tau}_1^-$) and a higher tau polarization for ($\tilde{e}_R^+ \rightarrow e^+ \tau^- \tilde{\tau}_1^+$). Several curves for the tau polarization ratio

$P(\tau^+)/P(\tau^-)$ are plotted against the stau mixing parameter $\cos \theta_{\tilde{\tau}}$ with different Δ values in Fig. 4(b). Varying the $r_{\tilde{B}}$ parameter could dramatically change the $\cos \theta_{\tilde{\tau}}$ dependence of $P(\tau^+)/P(\tau^-)$. We plot $P(\tau^+)/P(\tau^-)$ for five choices $r_{\tilde{B}} = 1.0, 1.5, 2.0, 2.5, 3.0$ in Fig. 4(c). As shown in the plot, the polarization ratio $P(\tau^+)/P(\tau^-)$ depends on $r_{\tilde{B}}$ sensitively when $0.3 \geq |\cos \theta_{\tilde{\tau}}| \geq 0.2$.

We can also study the neutralino mixing effects on the tau-lepton polarizations. Figure 5 shows typical plots in both the B -ino-like lightest neutralino scenario and in the Higgsino-mixed neutralino region with the model parameters $m_{\tilde{e}_R} = 200$, $|\mu| = 300$, $m_1 = 400$, $m_2 = 800$ GeV, and $\tan \beta = 10$. By comparing Fig. 5 to Fig. 3(a), we find that the tau polarization behavior in the Higgsino-mixed neutralino scenarios may look similar to that in the B -ino-like lightest neutralino scenarios with a larger $|\cos \theta_{\tilde{\tau}}|$ value. For instance, the tau polarization in the Higgsino-mixed neutralino region with $\cos \theta_{\tilde{\tau}} = -0.1$ would look like the tau polarization in the B -ino-dominant lightest neutralino scenario with $\cos \theta_{\tilde{\tau}} \approx -0.3$.

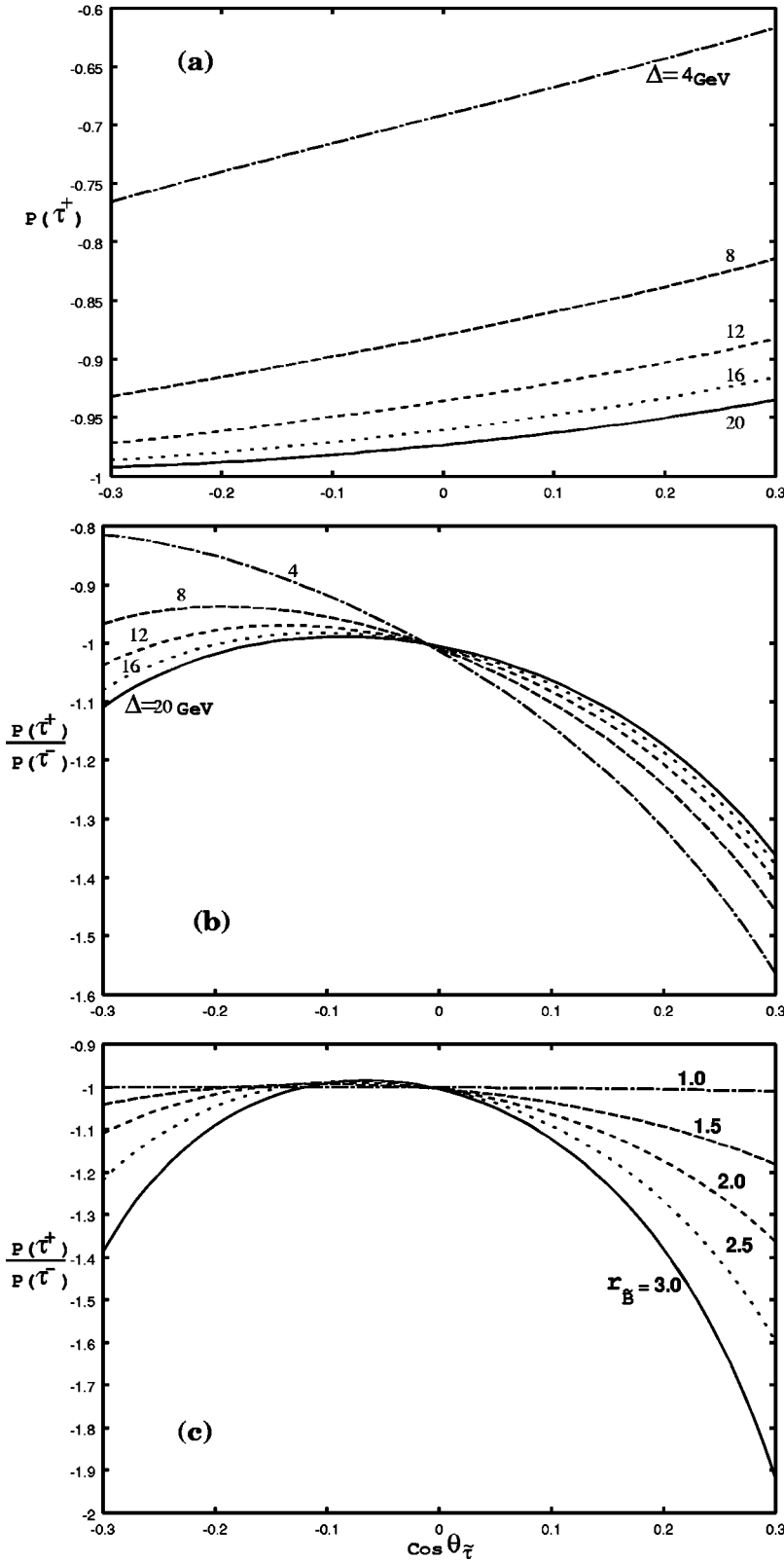


FIG. 4. (a) Tau polarization as a function of $\cos \theta_{\tilde{\tau}}$ for $r_{\tilde{B}}=2$ and five choices $\Delta=4, 8, 12, 16,$ and 20 GeV for the selectron decay $e_R^+ \rightarrow e^+ \tau^+ \tilde{\tau}_1^-$. (b) The ratio $P(\tau^+)/P(\tau^-)$ as a function of $\cos \theta_{\tilde{\tau}}$ for $r_{\tilde{B}}=2$ and five choices $\Delta=4, 8, 12, 16,$ and 20 GeV. (c) The ratio $P(\tau^+)/P(\tau^-)$ for $\Delta=20$ GeV and five choices $r_{\tilde{B}}=1.0, 1.5, 2.0, 2.5, 3.0$.

In Fig. 6 we plot the normalized distributions for the final state electrons and tau leptons as functions of their transverse momenta p_T in the selectron rest frame. Here we choose the model parameters $m_{\tilde{e}_R} = 200$ GeV, $r_{\tilde{B}} = 1.2$, $\cos \theta_{\tilde{\tau}} = -0.15$. We plot three different values of $\Delta = 12, 16, 20$ GeV, respectively. As seen from the figure, the peak values occur at

about $p_T = 7.5, 5.8, 4.3$ GeV (6.0, 4.9, 3.7 GeV) for the final state tau lepton (electron) distributions as we vary the Δ from 20, 16, to 12 GeV accordingly. It should be noticed that when the mass difference Δ is too small, the final state tau may be too soft to detect and the determination of the tau polarization would be a challenge. However, if the mass

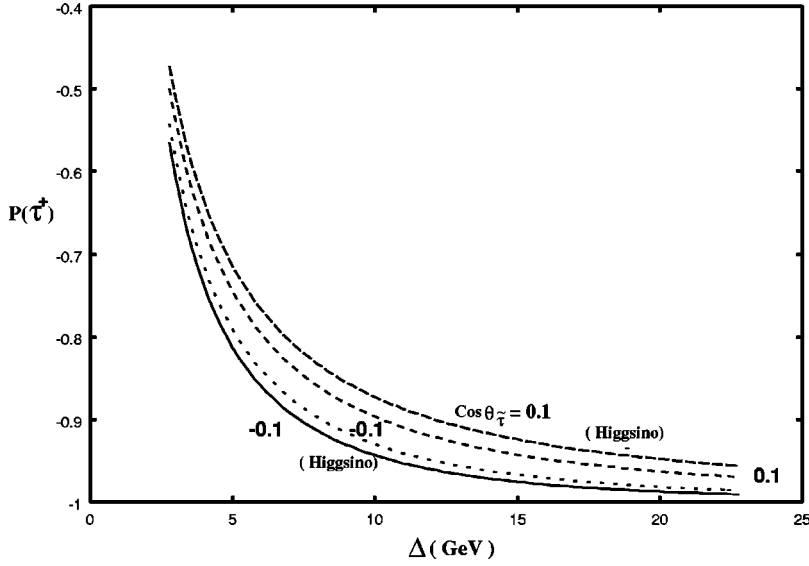


FIG. 5. The dependence of tau polarization on the mass difference $\Delta \equiv m_{\tilde{e}_R^-} - m_{\tilde{\tau}_1^-}$ with different $\cos \theta_{\tilde{\tau}}$ values. Curves are plotted both in the B -ino-like neutralino scenario and in the Higgsino-like neutralino scenario for the decay process $e_R^+ \rightarrow e^+ \tau^+ \tilde{\tau}_1^-$. Here we choose the model parameters $m_{\tilde{e}_R^-} = 200$, $|\mu| = 300$, $m_1 = 400$, $m_2 = 800$ GeV, and $\tan \beta = 10$.

splitting is large enough, the polarization of the final state tau lepton can be measured.

According to the numerical results the knowledge of the tau polarization in the three-body slepton decays can provide another observable and may help to reveal the stau mixing angle and/or the B -ino-slepton mass ratio $m_{\tilde{B}}^-/m_{\tilde{e}_R^-}$ in the small mass difference $\Delta \ll m_{\tilde{e}_R^-}$ limit. Experimentally, there may be a way for measuring the polarized tau-lepton productions in the selectron decay by observing its subsequent tau decays $\tau^- \rightarrow \pi^- \nu_\tau$ and $\tau^+ \rightarrow \pi^+ \bar{\nu}_\tau$. The tau polarizations can be obtained by measuring the spectrum of E_{π^\pm}/E_{τ^\pm} in the decays.

IV. CONCLUSION

In this paper we investigated the tau polarizations for the three-body slepton decays under the stau NLSP scenarios in the small mass difference limit $\Delta \ll m_{\tilde{e}_R^-}$. The exact formulas for calculating the slepton decay rates at the tree level are provided in Sec. II.

The measurements of tau lepton polarizations in the slepton decays provide another window for studying the SUSY model parameters. In the right-handed $\tilde{\tau}_R$ limit, the tau asymmetry ratio P_τ is solely determined by the mass difference parameter Δ . Numerical studies show explicit dependence on the stau mixing angles and/or the mass ratio $m_{\tilde{B}}^-/m_{\tilde{e}_R^-}$.

We also studied the distributions of the final state electrons and tau leptons as functions of their transverse momenta p_T in the selectron rest frame. The energy spectrum of the final state leptons are mainly determined by the mass difference ratio $\Delta \equiv m_{\tilde{e}_R^-} - m_{\tilde{\tau}_1^-}$. In our chosen parameters $m_{\tilde{e}_R^-} = 200$ GeV, $r_{\tilde{B}} = 1.2$, $\cos \theta_{\tilde{\tau}} = -0.15$ as we vary Δ from 12, 16 to 20 GeV, the peaks of the distributions range from $p_T = 4.3, 5.8$ to 7.5 GeV, respectively. However, if the mass difference is too small, the final state tau lepton will be too soft and the measurement of the polarization would be very difficult. But if Δ is large enough such that we can measure its polarization, the knowledge of tau-lepton polarization may help in determining the parameter space of a typical GMSB model.

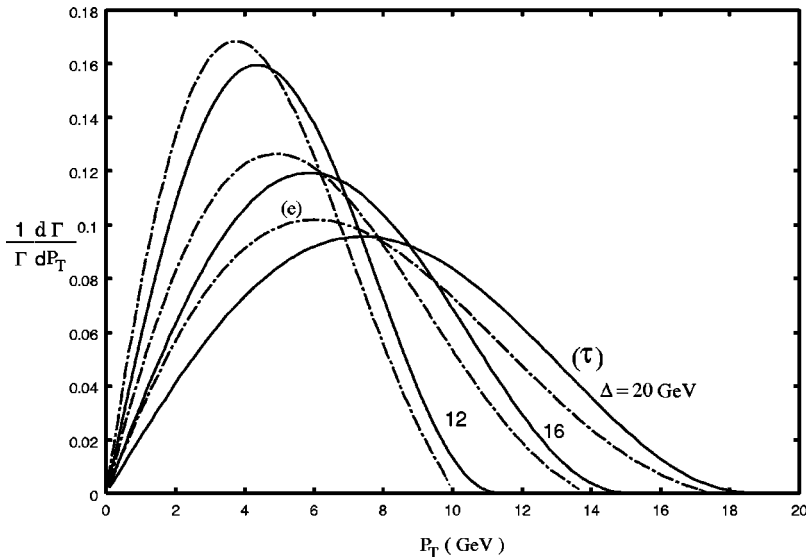


FIG. 6. Lepton p_T distributions in the rest frame of the \tilde{e}_R^+ decaying to $e^+ \tau^+ \tilde{\tau}^-$. Normalized p_T distributions for final e (dot-dash lines) and τ (solid lines) for the model parameters with $m_{\tilde{e}_R^-} = 200$ GeV, $\cos \theta_{\tilde{\tau}} = -0.15$, $r_{\tilde{B}} = 1.2$, and $\Delta = 12, 16, 20$ GeV, respectively.

ACKNOWLEDGMENTS

C.-L. Chou thanks M. E. Peskin for introducing the topic and useful discussion in the early stage of this work. C.-H.

Chou thanks S.-C. Lee for helpful discussions. This work was supported in part by the National Science Council of Taiwan (Grant No. NSC89-2112-M-001-070 and NSC89-2811-M-001-0100).

-
- [1] S. Dimopoulos and H. Georgi, Nucl. Phys. **B193**, 150 (1981); S. Dimopoulos, S. Raby, and F. Wilczek, Phys. Rev. D **24**, 1681 (1981); H. E. Haber and G. L. Kane, Phys. Rep. **117**, 75 (1985).
- [2] R. Arnowitt, P. Nath, and A. H. Chamseddine, *Applied N=1 Supergravity* (World Scientific, Singapore, 1984).
- [3] E. Cremmer, P. Fayet, and L. Gardello, Phys. Lett. **122B**, 41 (1983); P. Fayet *ibid.* **69B**, 489 (1977); **84B**, 241 (1979).
- [4] M. Dine, A. E. Nelson, and Y. Shirman, Phys. Rev. D **51**, 1362 (1995); M. Dine, A. E. Nelson, Y. Nir, and Y. Shirman, *ibid.* **53**, 2658 (1996).
- [5] S. Ambrosanio, G. L. Kane, G. D. Kirbs, and S. P. Martin, Phys. Rev. D **54**, 5395 (1996); S. Ambrosanio, G. D. Kirbs, and S. P. Martin, *ibid.* **56**, 1761 (1997).
- [6] M. Chen, C. Dionisi, M. Martinez, and X. Tata, Phys. Rep. **159**, 201 (1988); H. Baer, M. Brhlik, R. Munroe, and X. Tata, Phys. Rev. D **52**, 5031 (1995).
- [7] S. Dimopoulos, M. Dine, S. Raby, and S. Thomas, Phys. Rev. Lett. **76**, 3494 (1996); S. Dimopoulos, S. Thomas, and J. D. Wells, Nucl. Phys. **B488**, 39 (1997).
- [8] J. Bagger *et al.*, "The Case for a 500-GeV $e^+ e^-$ Linear Collider," hep-ex/0007022.
- [9] S. Ambrosanio, G. D. Kribs, and S. P. Martin, Phys. Rev. D **56**, 1761 (1997).
- [10] S. Ambrosanio, G. D. Kribs, and S. P. Martin, Nucl. Phys. **B516**, 55 (1998).
- [11] M. E. Peskin, Int. J. Mod. Phys. A **13**, 2299 (1998).